Moroccan Journal of Chemistry
ISSN : 2351-812X

Mor. J. Chem., 2023, Volume 11, Issue 3, Page 832-853
https://revues.imist.ma/index.php/morjchem
https://doi.org/10.48317/IMIST.PRSM/morjchem-v11i3.40080

Simultaneous adsorption of cationic and anionic dyes by raw pomegranate peel: Modelling of equilibrium, kinetical and thermodynamical studies

Wafae Abbach[1], Charaf Laghlimi[1] Jalal Isaad[1]
[1] *ERCI2A, FSTH, Abdelmalek Essaadi University, Tetouan, Morocco;*
Charaf.cac.fbs@gmail.com; j.isaad@uae.ac.ma

Received *08 May 2023,*
Revised *03 July 2023,*
Accepted *08 July 2023*

Citation*: Abbach W., Laghlimi C., Isaad J. (2023) Simultaneous adsorption of cationic and anionic dyes by raw pomegranate peel: Modelling of equilibrium, kinetical and thermodynamical studies, Mor. J. Chem., 14(3), 832-853*

Abstract: In this work, Raw Pomegranate Peel (RPP) was used as an adsorbent or the removal of anionic: Eriochrome black (EBT), Direct Blue (DB71) and cationic: Malachite green (MG), Methylene blue (MB) dyes from water. FT-IR spectroscopy showed that RPP has (-OH) and (-COOH) functional groups. The RPP powder shows an adsorption capacity of 81% for MB and 83% for MG obtained at pH= 7, and 69 % for DB71 and 62 % for EBT at pH3, in 60 min of contact for an initial dye concentration of 50 mg.L^{-1} and an amount of RPP of 0.1 g at a temperature of 298 k. The results of the isothermal analysis indicate that the Langmuir isothermal model described the adsorption of the studied dyes on RPP, and the sorption kinetics data are consistent with the pseudo-second-order model. The adsorption on a solution simulating real conditions shows a promising application in wastewater treatment.

Keywords: Dye; Adsorption, pomegranate peel, Water, Recycling.

1. Introduction

The use of refractory chemicals in various human activities such as the chemical industry, agriculture, dyeing process, etc., results in the discharge of a large amount of polluted water rich in chemicals generally toxic. Among these chemical compounds, dyes are used extensively and emitted directly in the environment (Yagub *et al*. 2014), (Bauer *et al*., 2001). In terms of health, there are a number of studies (Anliker *et al*., 1979; Chung *et al*., 1981) have demonstrated the potentially toxigenic and carcinogenic actions of organic dyes., as well as their high chemical and photochemical stability. The toxicity of dyes is related to the presence of carcinogenic substituents in their chemical structure, such as cyanides, aromatic nuclei, barium salts, and halogens (especially Cl) which are generally highly reactive towards the nitrogenous bases of DNA and RNA, which deteriorates the genetic code of the cell and the appearance of severe health damages such as mutations and cancers (Zollinger *et al*., 1991; Tsuda *et al*., 2000; Combes *et al*., 1982; IARC International Agency for research on cancer., 1982). Therefore, the effluents containing these dyes have to be treated before any release into the environment. In this sense, a large number of physical (Wawrzkiewicz *et al*., 2022; He *et al*., 2022; Isaad *et al*., 2022; Liu *et al*., 2022; Kankou *et al*., 2021), chemical (Liao *et al*., 2022; Lia *et al*., 2022; Li *et al*., 2022; Xu *et al*., 2022; Xiang *et al*., 2022), photochemical (Hunger *et al*., 2003; Ahmad *et al*., 2022; Hu *et al*., 2022; Lee *et al*., 2022; Athawale *et al*., 2020), and electrochemical (Liu *et al*., 2022; Sun *et al*., 2022; Shokri *et al*., 2022; Cui *et al*., 2021; Hamous *et al*., 2021) processes, as well as the water-solubilization of organic dyes by grafting carbohydrates onto the starting dyes (Bianchini *et al*.,

2007), (Isaad *et al*., 2009), (Bianchini *et al*., 2012), (Isaad *et al*., 2013), (Isaad *et al*., 2020), (Bianchini, *et al*., 2008), have been used to treat and reduce the environmental impact of water polluted by dyes. Most of the materials used in these dye removal processes are of high dye adsorption performance. However, the preparation of these materials involves a number of toxic chemicals, which can induce secondary environmental contamination. Therefore, there is a great interest in the eco-design of adsorbent materials using no or few toxic substances. In this context, many works have indicated that adsorbents based on biopolymers (Druet *et al*., 2015; Medjahed *et al*., 2013; Sheth *et al*., 2021; Ben Ali *et al*., 2017; Al-Onazi *et al*., 2021; Bellahsen *et al*., 2021; Isaad *et al*., 2021; Elsherif *et al*., 2022) and agro-wastes (Eltaweil *et al*., 2021; Salmani *et al*., 2021; Akram *et al*., 2022; Muhammad *et al*., 2020; Kyzas *et al*., 2017; Gündüz *et al*., 2017; Usman *et al*., 2022; Haque *et al*., 2020) are effective in removing several pollutants in general, such as heavy metals (Druet *et al*., 2015; El Hammari *et al*., 2023; Sheth *et al*., 2021; Ben Ali *et al*., 2017; Al-Onazi *et al*., 2021; Bellahsen *et al*., 2021), anions (Isaad *et al*., 2021) wastes (Eltaweil *et al*., 2021; Salmani *et al*., 2021; Akram *et al*., 2022), and dyes wastes (Eltaweil *et al*., 2021; Salmani *et al*., 2021; Akram *et al*., 2022). Agricultural wastes are naturally renewable materials, available in large quantities, cheaper and better than other materials used as adsorbents due to their usual use without or with minimal processing (washing, drying, grinding), which can reduce the economic cost of producing an adsorbent from agricultural waste as a raw product and minimize the cost of energy in the thermal process of treatment. Pomegranate is one of the most popular fruits in the world and is widely consumed in the food industry, which generates a considerable quantity of pomegranate peel as a by-product and is therefore inexpensive. Several bio-adsorbents based on RPP (Ben-Ali *et al*., 2022), or calcined pomegranate peel (CPP) (Eltaweil *et al*., 2021; Salmani *et al*., 2021), were performed for removing dyes from aqueous media. CPP-based bio-adsorbents are effective in removing dyes, however, their preparation is done at high temperatures (400-800 °C), which increases their economic cost and decreases their ecological interest. On another side, it is important to note that only one type of dye (anionic or cationic) is used to study the adsorption capacity of dyes by RPP, and to our knowledge, the use of adsorbents based on RPP to remove a mixture of dyes with a different chemical nature is rather limited in the literature. Removal of Eriochrome black (EBT), Direct Blue (DB71), Malachite green (MG) and Methylene blue (MB) received more attention by researchers (Aaddouz *et al*., 2023; Kouar *et al*., 2021; Loubna *et al*., 2019; Dahri *et al.* 2018; El Badraoui *et al*., 2019). Therefore, the above limitations indicate (1) great interest in using RPP as a natural biosorbent and (2) investigating the ability of this material for removing a cationic and anionic dye mixture (anionic: EBT, DB71 and cationic: MG, MB) from an aqueous solution. In this work, RPP was used as a promising bio-adsorbent to remove both anionic and cationic dye from aqueous media with an easy and inexpensive preparation method, as well as to improve the efficiency of the adsorption process.

2. Methodology

2.1 Reagents and chemical solutions

All the chemical compounds are of reagent quality (Aldrich Chemical - France.) and were used without purification. The pomegranates used in this study are of the "Safri" variety collected from the Ouled Abdellah region (Fqih Ben Salah province - Morocco). Four dyes (**Figure 1**) were chosen for the study of the adsorption capacity of RPP. All the experimental procedures of this study are described in the supporting information section.

2.2 Preparation of the adsorbent

Pomegranate peels were collected, dried in the air, and then crushed in a mechanical crusher. In order to remove dust, soluble impurities, coloring matters, and water-soluble tannins, the obtained powder was washed with distilled water and then boiled for one hour at 90°C several times until the supernatant was colorless. The resulting powder was dried at 100°C until a constant weight was achieved. The dried biomaterial was then grounded through increasingly fine sieves to obtain a powder of different particle sizes. The prepared bio-adsorbents RPP were characterized by elemental analysis, FTIR, TG/DTA, XRD, Boehm titration, B.E.T analysis, and point of zero charges (pH_{pzc}) analysis.

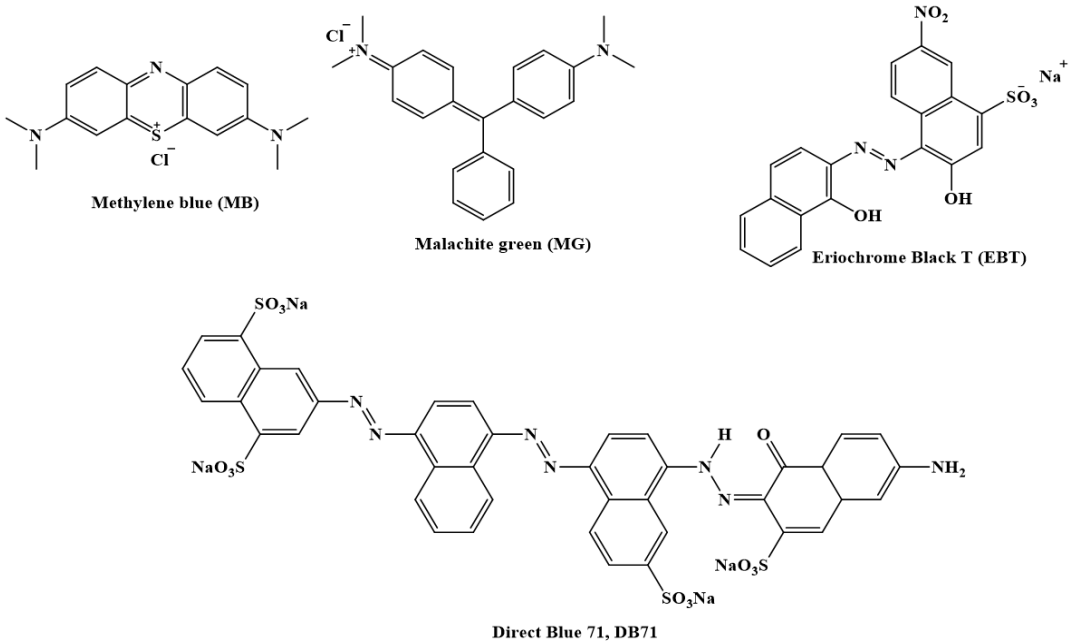

Figure 1: Chemical structure of the studied dyes

3. Results and Discussion

3.1 Characterization of the RPP as bio-adsorbent

3.1.1. Elemental analysis

The elemental analysis of RPP (**Table 1**) shows that RPP contains carbon (42.42%) and oxygen 51.66%, as well as a measurable amount of hydrogen (5.90 %). This chemical composition is in agreement with the literature where plant waste is mainly composed of lignin, cellulose, and hemicellulose (Malik, *et al*., 2017).

Table 1: Elemental composition of RPP.

Chemical composition	(wt. %)
Carbon	42.42
Oxygen	51.66
Hydrogen	5.92

3.1.2. FT-IR spectroscopy

The FT-IR spectrum of RPP (**Figure 2**) showed characteristic bands at 3435 and 2906 cm^{-1} attributed to COOH, O-H (aliphatic or aromatic), and C-H groups (Ben-Ali *et al*., 2022) respectively. The vibrations that appeared at 1751 and 1633 cm^{-1} confirmed the presence of C=O groups (aldehyde,

ketone, carboxylic acid, and acetate). The other absorption bands appearing at 1447, 1383, 1181 cm^{-1}, and 1060 cm^{-1} are assigned to -C-OH, -O-H, -C-O, and -C=O respectively. The band at 1600 cm^{-1} is attributed to the ionized O=C-O^- groups (Malik, *et al*., 2017). These results are in agreement with the nature of the chemical functions present on the surface of RPP and identified by titration according to the Boehm method. Therefore, RPP contains a high number of OH and COOH functions on its surface, which can potentially interact with the dyes.

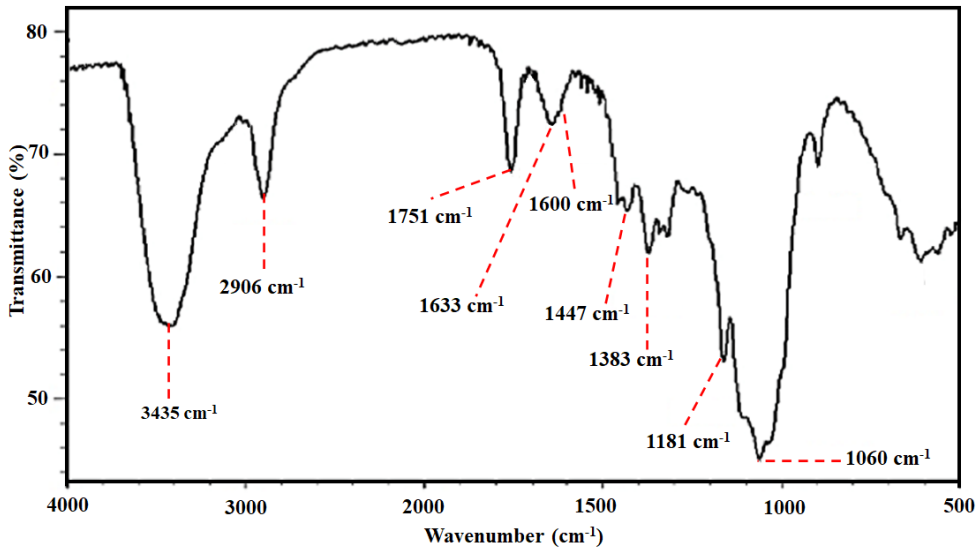

Figure 2: FT-IR data of RPP

3.1.3. Thermogravimetric analysis

The DTG spectrum (**Figure 3**) of RPP shows a first weight loss observed between 50 and 180 C° which may be due to the dehydration of volatiles. Three other significant losses are observed due to the decomposition of hemicelluloses (180 - 350 °C), cellulose (350 - 500 °C), and lignin (380 - 600 °C).

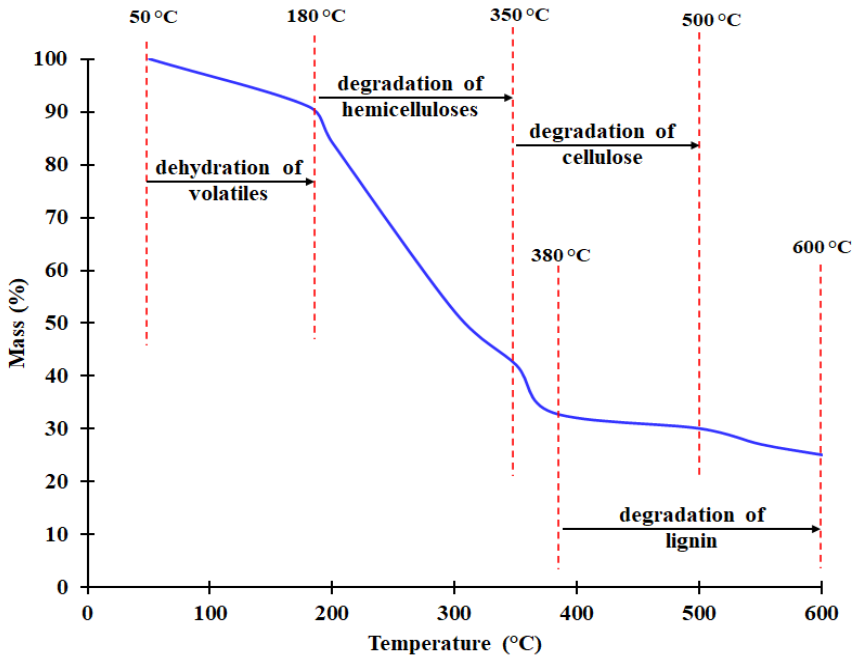

Figure 3: DTG spectrum of RPP

3.1.4. XRD analysis

The X-ray diffraction spectrum (**Figure 4**) of RPP shows a single, and very broad peak at 2θ = 20.57, suggesting that RPP has an amorphous structure. This result is also supported by the literature in which agricultural wastes are generally characterized by an amorphous structure (Vinod, *et al*., 2010).

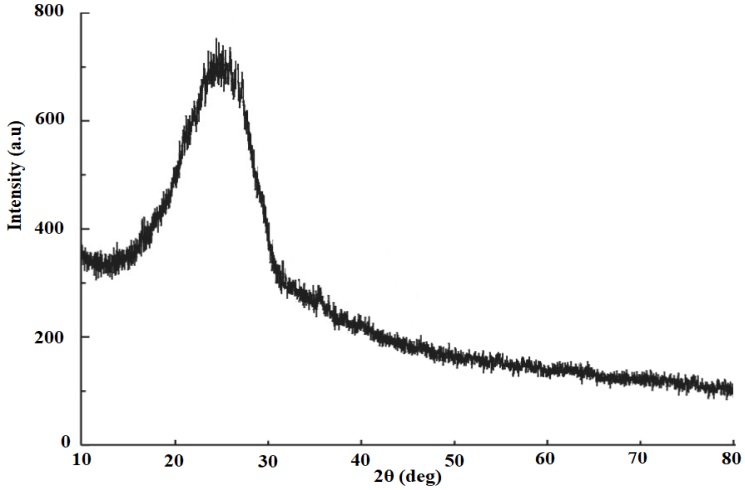

Figure 4: XRD spectrum of RPP

3.1.5. B.E.T surfaces analysis

The specific surface area was measured for RPP powders of different sizes. **Table 2** indicates that the specific surface area increases from 0.042 $m^2.g^{-1}$ to 1.105 $m^2.g^{-1}$ when the size of the particles decreases from 800 to 250 µm. On the other hand, particles of 250 µm present a total volume and an average pore diameter in the range of 0.0017 $cm^3.g^{-1}$ and 71.45 Å respectively. These textural properties suggest that the RPP powder can be considered a mesoporous material of type IV according to IUPAC.

Table 2: Specific surface area of RPP.

Particle size (µm)	Specific surface area ($m^2.g^{-1}$)
250	1.105
315	0.064
800	0.042

3.1.6. Zeta potential

The zeta potential of RPP (**Figure 5**) shows that the particles of RPP present an isoelectric point (pH_{pzc}) around pH_{pzc} = 5.6. At pH < pH_{pzc}, the surface of RPP has a positive charge and the zeta potential reaches a value of +24 mV at pH = 3. In contrast, at pH>pHpzc, the surface of RPP presents a negative charge, and its zeta potential reaches values of -20, and -19 mV at pH 10 and 11 respectively. The changes in the electrical charges of RPP particles with pH are due to the carboxylic (-COOH) and hydroxylic (-OH) groups present in abundance in RPP. Indeed, at pH > pH_{pzc}, the RPP particles show a negative charge due to the ionization/deprotonation of the carboxylate and alcoolate functions to carboxylate $-COO^-$ and alcoolate $-O^-$. However, at pH < pH_{pzc}, the -COOH, and -OH groups are protonated and the RPP particles become positively charged. According to the zeta potential results, at pH > pH_{pzc}, the adsorption of cations is favored as the RPP surface is negatively charged due to

deprotonation, while at pH < pH_{pzc}, the electric charge on the surface of RPP is positive, and the anions adsorption is favorited. In this case, adsorption of anionic and cationic dyes by RPP should be appropriate when solution pH is below 5.6, and above 5.6 respectively, due to electrostatic dye-charge interactions with RPP.

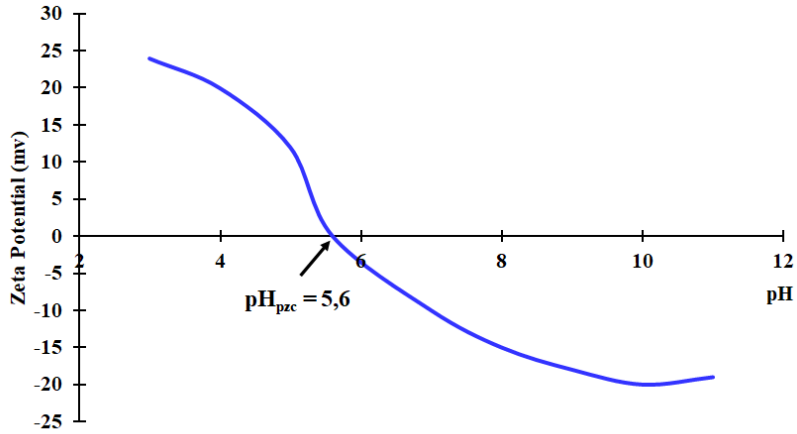

Figure 5: Zeta potential values of RPP versus pH.

3.2. Dyes adsorption capacity studies

3.2.1. Effect of initial pH

The pH of the solution of adsorption is an important parameter affecting the adsorption capacity of the RPP bio-adsorbent for anionic (EBT, DB71) and cationic (MG, MB) dyes. In fact, the electric charge of the dyes and the adsorbent changes according to the pH of the adsorption solution. For this reason, the adsorption capability of RPP to remove the dyes was studied at a pH between 2 and 11. As reported in **Figure 6**, The adsorption of cationic dyes (MB, MG) is weak in an acidic medium. When the pH increases, the removal rate increases up to a maximum value of 81% for MB and 83% for MG obtained at pH= 7. On the other hand, in the case of anionic dyes (EBT, DB71), the removal rate reaches a maximum value of 69% for DB71 and 62% for EBT at pH3 which decreases with the increase of the pH of the solution.

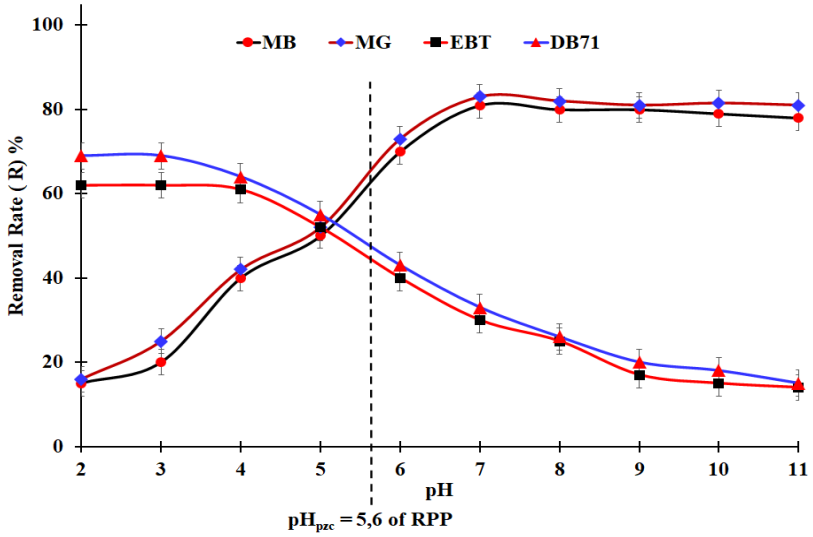

Figure 6: Adsorption capacities of RPP towards the anionic (EBT, DB71) and cationic (MG, MB) dyes as a function of pH. Conditions: C_{dye} = 50 mg.L^{-1}; $V_{Solution}$ = 100 mL; Adsorbent dosage = 0.10 g; Temperature = 25°C; Contact time = 120 min.

The pH effect of the adsorption solution on the removal performance of RPP towards anionic (EBT, DB71) and cationic (MG, MB) dyes depends on the value of pH_{pzc} = 5.6 and on the ionization state of the functional groups available on the surface of the RPP powder. In fact, at pH < pHpzc, the (-OH, -COOH) groups are protonated to ($-OH_2^+$, $CO_2H_2^+$) which renders the surface of RPP with a positive charge allowing greater electrostatic attractiveness towards the anionic dyes (EBT, DB71). On the other hand, at pH>pHpzc, the functional groups (-OH, -COOH) are deprotonated to ($-O^-$, COO^-) and the RPP surface becomes a negative charge, which favors the adsorption of cationic dyes (MB, MG). These results confirm that RPP is effective in adsorbing dyes over a wide pH range, regardless of their electrical charge. The adsorption of the studied dyes on RPP was confirmed by recording the XPS spectrum of RPP and RPP/dye. As shown in **Figure 7a**, the XPS spectrum of RPP shows sharp peaks at 285 eV and 532 eV corresponding to C1s and O1s, respectively. After dye adsorption, new peaks appear at 400 eV and 167.4-168.2 eV which are assigned to N1s (**Figure 7b**) and S2p (**Figure 7c-e**) of the dyes.

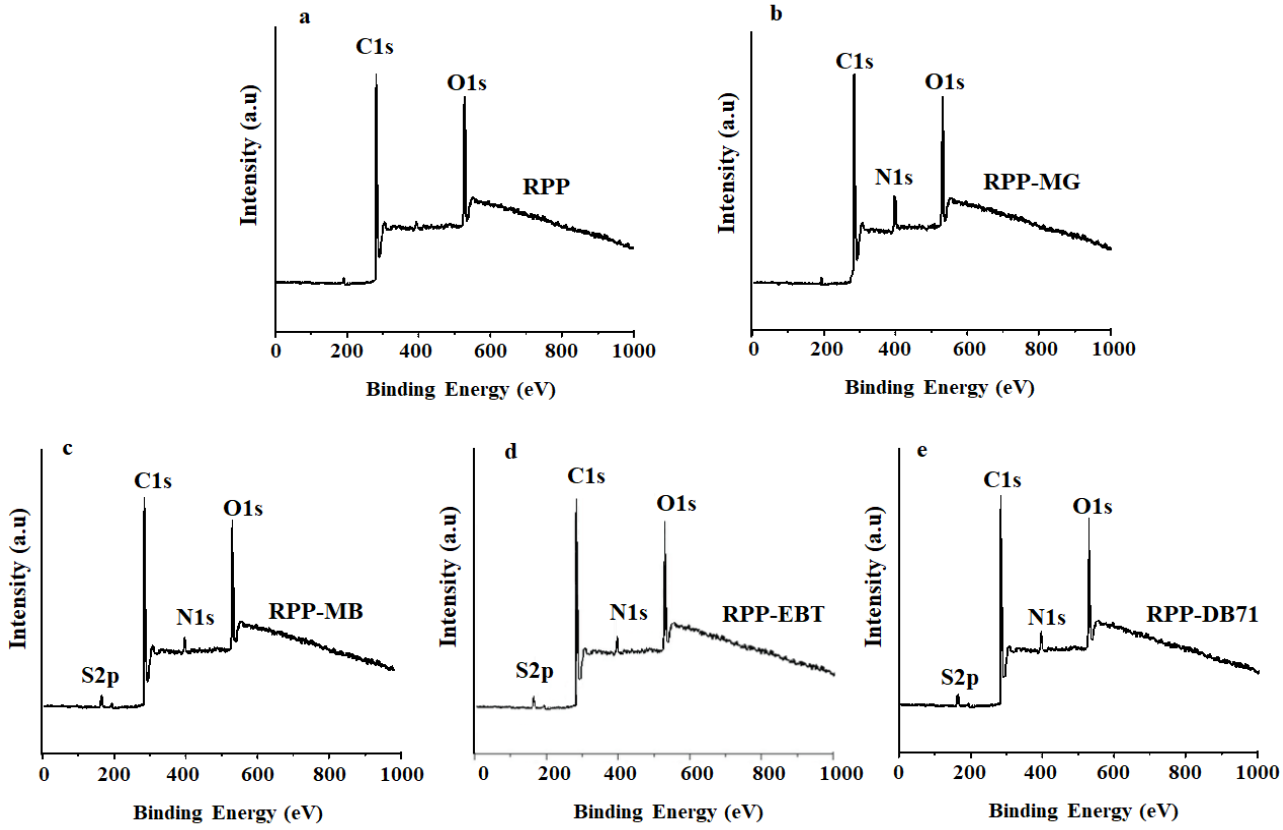

Figure 7: XPS spectra of RPP (a) before and (b-e) after dye adsorption

3.2.2. Effect of temperature

The temperature effect on the adsorption of the anionic (EBT, DB71) and cationic (MG, MB) dyes on RPP was studied by varying the temperature of the adsorption experiment at 298, 313, 333, and 353 K. **Figure 8** shows that the removal rate decreased slightly from 71% to 59% for MG, from 80% to 56% for MB, from 81% to 67% for EBT, and from 88% to 74% for DB71 by increasing the temperature from 298 to 353 K. These results suggest that the physical binding strength between the dye and the -COOH and -OH groups of RPP decreases slightly with the increase in temperature. Consequently, RPP has the potential to be used over a large temperature range for the adsorption of both anionic (EBT, DB71) and cationic (MG, MB) dyes.

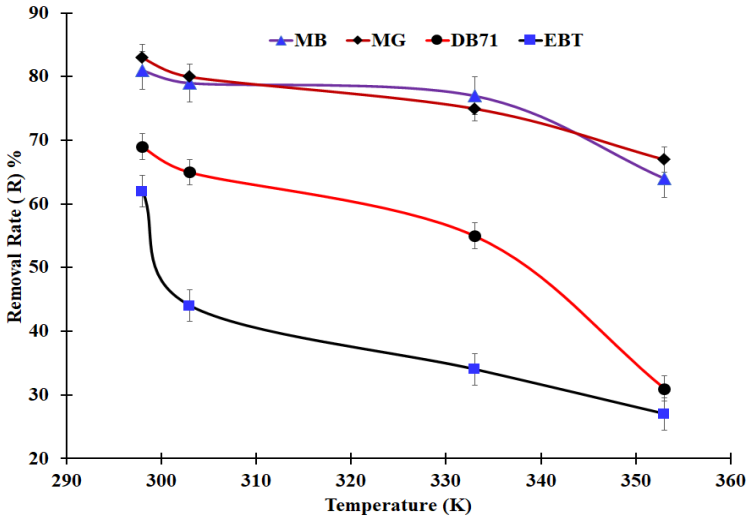

Figure 8: Effect of the temperature on the adsorption of the anionic (EBT, DB71) and cationic (MG, MB) dyes into RPP. C_{dye} = 50 mg.L^{-1}; $V_{Solution}$ = 100 mL; Adsorbent dosage = 0.10 g; pH = 3 (for EBT, DB71) and 7 (for MG, MB); Contact time = 60 min.

3.2.3. Effect of the initial dye concentration

The effect of initial dye concentration was studied using 20, 60, 80, 100, and 150 mg.L^{-1} as initial concentrations and at different periods. As shown in **Figure 9**, increasing the initial concentration of dye increases the dye adsorption capability (q_e), which is in accordance with the literature (Isaad *et al.*, 2021).

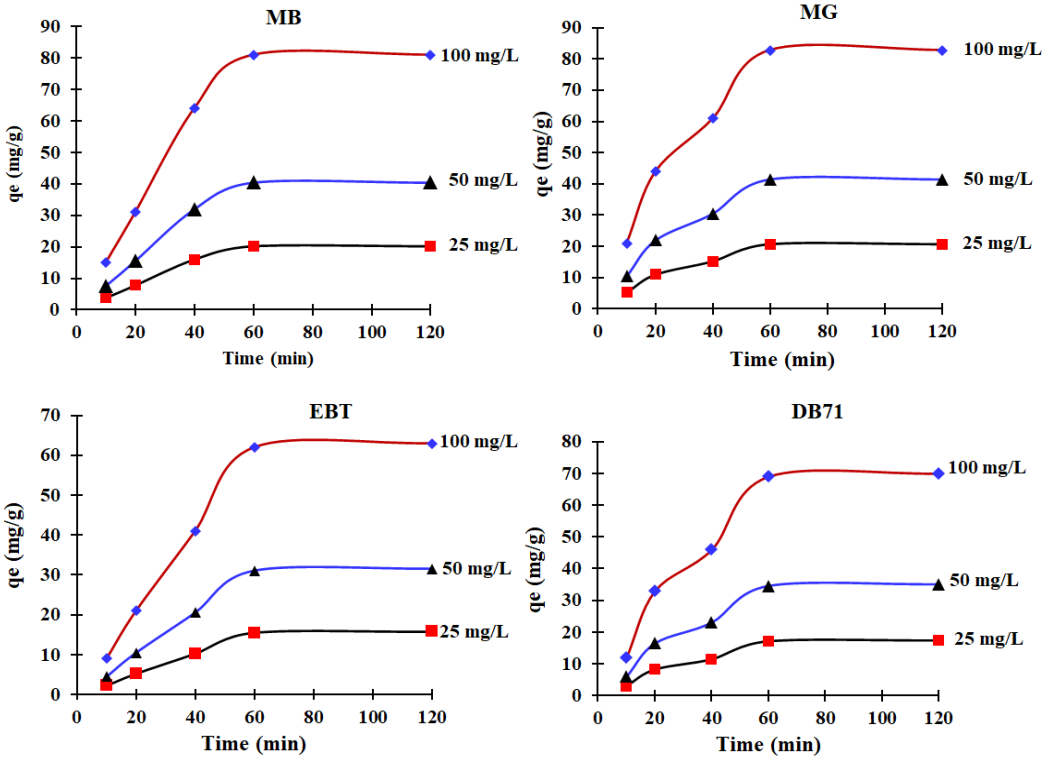

Figure 9: Effect of the initial dye concentration on the adsorption of the anionic (EBT, DB71) and cationic (MG, MB) dyes into RPP. $V_{Solution}$ = 100 mL; Adsorbent dosage = 0.10 g; pH = 3 (for EBT, DB71) and 7 (for MG, MB). Contact time = 60 min, Temperature 25 °C.

The adsorption capacity of RPP has doubled or tripled with a dye concentration of 100 $mg.L^{-1}$ for 60 min compared to the low concentration of 25 $mg.L^{-1}$. In fact, increasing the initial dye concentration results in rapid dye diffusion in the RPP, and strong dye adsorption, however, equilibrium is reached after a relatively long time. These results may be attributed to the increase in the concentration gradient force upon increasing the initial dye concentration, which implies favoring the intra-particle diffusion (Isaad, *et al*., 2021). Thus, these results demonstrate the main role of initial dye concentration in dye adsorption in RPP powder, which can exhibit strong dye adsorption at high and low levels of dye concentration.

3.2.4. Effect of ionic strength

The effect of NaCl quantity on the ability of RPP to remove anionic (EBT, DB71) and cationic (MG, MB) dyes was studied by adding different concentrations of NaCl (from 0 to 2 $g.L^{-1}$) to the solution in the adsorption experiments. As shown in **Figure 10**, dye retention decreased with increasing NaCl concentration up to 1 $g.L^{-1}$, and beyond this value, the retention rate (R) remained stable. These results can be explained by the occupation of charged sites on the surface of the RPP by Na^+ and Cl^- ions, which reduce the number of free charged sites available to adsorb dyes on the RPP surface through electrostatic dye-charge interactions with the RPP. In this sense, the addition of NaCl to a dye solution increases the amount of Cl^- and Na^+ ions, resulting in competition between Cl^-, Na^+, and dye ions for active cationic and anionic binding sites in the RPP. As the amount of NaCl increases, Cl^- and Na^+ ions gradually substitute for the dye up to 1 $g.L^{-1}$, after which equilibrium is reached between Cl^-, Na^+, and their corresponding ionic forms of the dye.

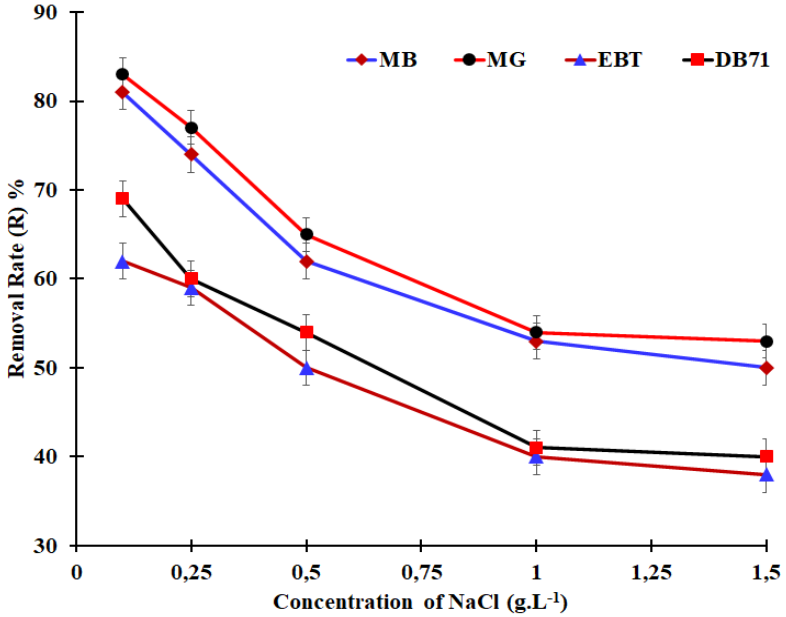

Figure 10: The effect of NaCl concentration on the removal of anionic (EBT, DB71) and cationic (MG, MB) dyes into RPP. Conditions: $V_{Solution}$ = 100 mL; RPP quantity = 0.10 g; pH = 3 (for EBT, DB71) and 7 (for MG, MB). Contact time = 60 min, Temperature= 25 °C.

3.2.5. Effect of the RPP quantity

In order to investigate the effect of the RPP quantity on the adsorption of the anionic (EBT, DB71) and cationic (MG, MB) dyes, the removal experiment was performed using different increased amounts of adsorbent (from 0.06 to 0.3 g) and constant dye concentration (50 $g.L^{-1}$). As shown in **Figure 11**, the removal rate (R) shows an increase with RPP quantity from 0.06 g to 0.1 g and then remains constant

from 0.1 to 0.3 g for all anionic (EBT, DB71) and cationic (MG, MB) dyes. These results may be due to the availability of more active sites capable of adsorbing dyes when a high quantity of RPP is used, thus increasing its removal efficiency (R).

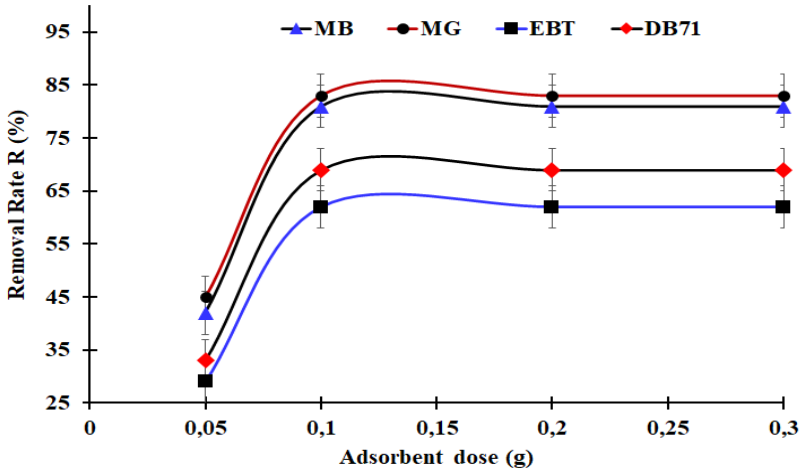

Figure 11: The effect of the RPP quantity on the removal of the anionic (EBT, DB71) and cationic (MG, MB) dyes. Conditions: C_{dye} = 50 mg.L^{-1}; $V_{Solution}$ = 100 mL; pH = 3 (for EBT, DB71) and 7 (for MG, MB). Contact time = 60 min, Temperature 25 °C.

3.2.6. Effect of Adsorbent size

The effect of adsorbent size on the adsorption capacities of the studied cationic and anionic dyes is presented in **Figure 12**. It shows that the removal rate of RPP increases when the adsorbent particle size is increased from 800 to 250 µm, leading to higher removal of the studied dyes. This result is quite expected considering that the RPP particles with the size of 250 µm have the highest specific surface area value (1.105 m^2.g^{-1}) compared to the other sizes (315 and 800 µm) and, therefore, the number of RPP active sites is very high on the surface of the RPP particles with the size of 250 compared to the other sizes (315 and 800 µm)

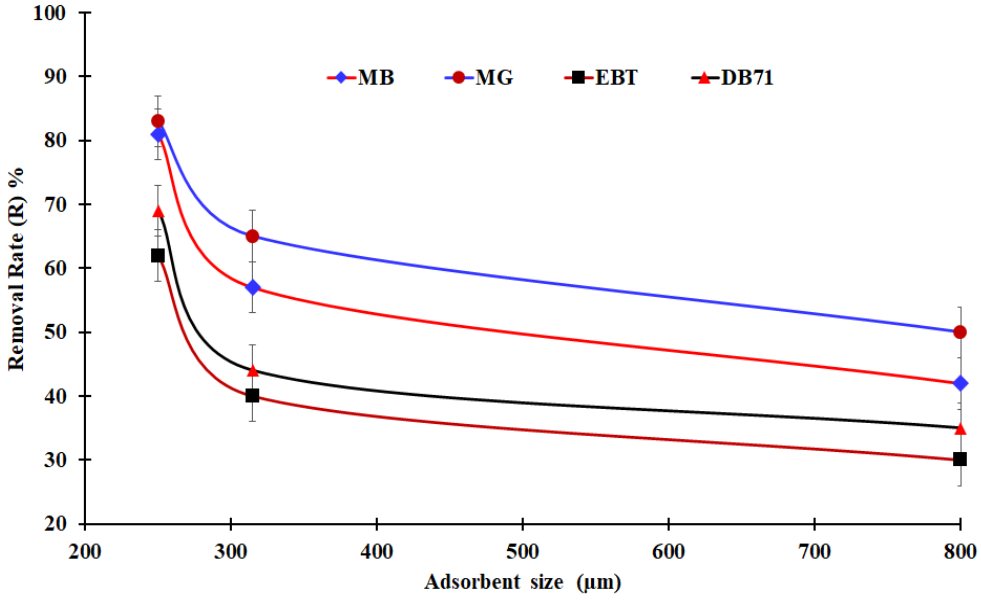

Figure 12: The effect of the adsorbent (RPP) size on the removal of the studied anionic (EBT, DB71) and cationic (MG, MB) dyes. Conditions: C_{dye} = 50 mg.L^{-1}; $V_{Solution}$ = 100 mL; pH = 3 (for EBT, DB71) and 7 (for MG, MB). Contact time = 60 min, Temperature 25 °C.

3.2.7. Effect of the contact time

The determination of the optimal contact time for the adsorption of anionic (EBT, DB71) and cationic (MG, MB) dyes onto RPP powder involves the calculation of the contact time, corresponding to an equilibrium state of saturation of the RPP by the dye. For this purpose, the adsorption experiments were performed under various contact times, and the results obtained given in **Figure 13** show that the removal rate of the dyes increases rapidly to an optimum value in the first 60 minutes and it remains approximately stable from 60 to 120 minutes, which indicates a stable equilibrium state. This result demonstrates that the equilibrium adsorption of the studied dyes into the RPP powder is very fast. Afterward, the adsorption becomes progressively slower. This is due to the presence of a high number of free adsorption sites available on the surface of the RPP powder during the initial adsorption phase. Consequently, these lead to the reduction of the removal rate, and after 60 min a plateau is established corresponding to the equilibrium state.

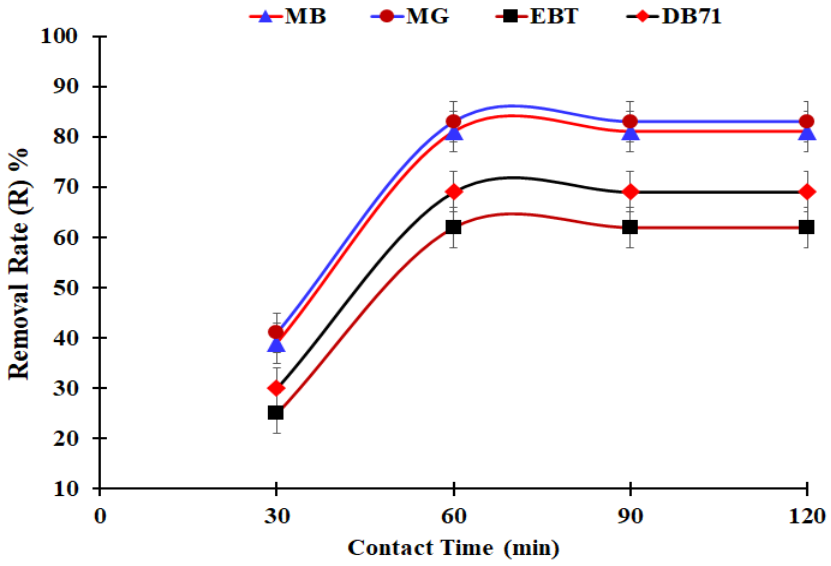

Figure 13: The effect of the contact time on the removal of the studied anionic (EBT, DB71) and cationic (MG, MB) dyes. Conditions: C_{dye} = 50 mg.L^{-}1; $V_{Solution}$ = 100 mL; pH = 3 (for EBT, DB71) and 7 (for MG, MB). Temperature 25 °C.

3.3. Adsorption kinetics

Sorption kinetics is of great interest for a wastewater treatment process. It provides major information about the reaction mechanism followed by the pollutant during its sorption onto the solid adsorbent. For this purpose, experimental data on adsorption kinetics were modeled using pseudo-first-order (Li *et al*., 1999) and pseudo-second-order (Ho *et al*., 1999) models. As shown in **Table 3**, the R^2 correlation coefficients (approximately 0.999) are greater than the R^2 values (less than 0.9912) of the pseudo-first-order model), indicating that the sorption kinetics of anionic (EBT, DB71) and cationic (MG, MB) dyes by RPP are consistent with the pseudo-second-order kinetic model. Furthermore, the experimental q_e(exp) values calculated on the basis of the pseudo-second-order model are approximately similar to the calculated q_e(exp) values compared to the corresponding values calculated from the pseudo-first-order equation. These results indicate that the adsorption of the dyes on the RPP powder implies chemisorption as well as physisorption.

Regarding the description of the mass transfer mechanism of adsorbates, the intra-particle diffusion model was tested to describe the adsorption of anionic and cationic dyes on RPP powder. As shown in Table 3, the coefficients calculated according to the intra-particle diffusion model, are in accordance

with this model. Moreover, **Figure 14** shows two linear parts in the curves of all studied dyes, indicating that adsorption occurs in two or more steps. Therefore, the intra-particle diffusion model can be used to describe the adsorption of anionic (EBT, DB71) and cationic (MG, MB) dyes in two steps. In the first step, the dye diffuses from the solution to the surface of the RPP powder, and the second step consists of a final equilibrium in which intra-particle diffusion is limited. Moreover, the correlation coefficient values for the dyes range from 0.951 to 0.977, confirming that the intra-particle diffusion model is appropriate to describe the first step of dye adsorption on RPP. However, the second stage of dye adsorption is slow and is characterized by the occupation of the majority of the active sites, making this stage the limiting one. On the other hand, the k1d constants of the cationic dyes (MG, MB) are higher than the constants of the anionic dyes (EBT, DB71), which indicates that the adsorption of cationic dyes is faster than that of anionic dyes.

Table 3: kinetic parameters of the studied anionic (EBT, DB71) and cationic (MG, MB) dyes onto RPP powder. Conditions: $V_{Solution}$ = 100 mL; pH = 3 (for EBT, DB71) and 7 (for MG, MB). Temperature 25 °C.

	Concentration of MG ($mg.L^{-1}$)			Concentration of MB ($mg.L^{-1}$)			Concentration of EBT ($mg.L^{-1}$)			Concentration of DB71 ($mg.L^{-1}$)		
	25	**50**	**100**	**25**	**50**	**100**	**25**	**50**	**100**	**25**	**50**	**100**
q_e (exp) $mg.g^{-1}$	20.75	41.5	83.17	20.25	40.51	81.21	15.51	31.22	62.05	17.25	34.5	69.23
Pseudo-first order												
k_1 (10^{-2})(min^{-1})	1.18	1.95	1.57	2.34	1.85	1.12	2.05	2.12	1.58	1.61	2.03	1.25
q_e cal ($mg.g^{-1}$)	19.85	40.28	84.12	19.13	39.34	78.99	15.11	33.54	6167	17.89	33.75	70.45
R^2	0.894	0.864	0.905	0.905	0.889	0.884	0.872	0.862	0.907	0.864	0.883	0.899
Pseudo-second order												
k_2 (10^{-3})($g.mg^{-1}.min^{-1}$)	2.55	1.82	1.58	3.41	1.75	2.22	3.38	2.08	2.98	1.78	2.52	3.11
q_e cal (mg. g^{-1})	20.12	41.64	81.08	19.34	41.12	79.55	14.89	30.38	60.97	17.11	31.21	67.75
R^2	0.984	0.991	0.988	0.99	0.974	0.982	0.973	0.977	0.971	0.982	0.985	0.976
Elovich												
A ($mg.g^{-1}$. min^{-1})	0.659	0.873	0.855	0.442	0.426	0.594	0.529	0.599	0.912	0.277	0.785	1.297
β ($g.mg^{-1}$)	0.992	0.842	0.693	5.694	2.547	1.634	2.257	1.507	1.273	4.324	2.264	1.504
R^2	0.945	0.951	0.937	0.954	0.952	0.942	0.952	0.943	0.922	0.939	0.958	0.936
Intra-particle diffusion												
K_1d ($mg.g^{-1}$. $min^{1/2}$)	0.577	0.917	1.364	0.431	0.672	0.941	0.551	0.602	0.687	0.307	0.710	0.847
C_1 ($mg.g^{-1}$)	11.25	22.25	45.52	11.34	19.64	39.52	8.16	13.92	34.82	9.75	15.42	38.52
R_1^2	0.951	0.959	0.961	0.955	0.960	0.958	0.977	0.967	0.962	0.953	0.964	0.973
K_2d ($mg.g^{-1}$. $min^{1/2}$)	0.064	0.071	0.095	0.075	0.081	0.089	0.052	0.074	0.088	0.075	0.091	0.097
C_2 ($mg.g^{-1}$)	19.11	38.95	81.25	20.12	40.68	78.66	15.04	30.362	59.96	16.11	32.34	67.58
R_2^2	0.656	0.759	0.665	0.712	0.689	0.598	0.687	0.687	0.723	0.698	0.711	0.658

3.4. Thermodynamics of adsorption

In general, the interactions between the dye and the adsorbent are strongly temperature dependent. For this reason, a thermodynamic study is necessary to investigate whether the adsorption of the studied dyes onto the PPR is feasible and also to evaluate its nature. In this thermodynamic study, ΔG°, ΔH°, and ΔS° were calculated at 303, 318, 328, and 343 K, and the obtained calculations are summarized in Table 4. ΔG shows negative values for all dyes, indicating spontaneous adsorption of the dyes onto the PPR powder. In addition, the ΔG values are low and they range from 0 to 20 kJ/mol, which implies physical adsorption based on electrostatic interactions between PPR and dye (Kavitha *et al*., 2007). On the other hand, the sorption of the dyes studied by PPR is considered exothermic based on the negative values of ΔH°.

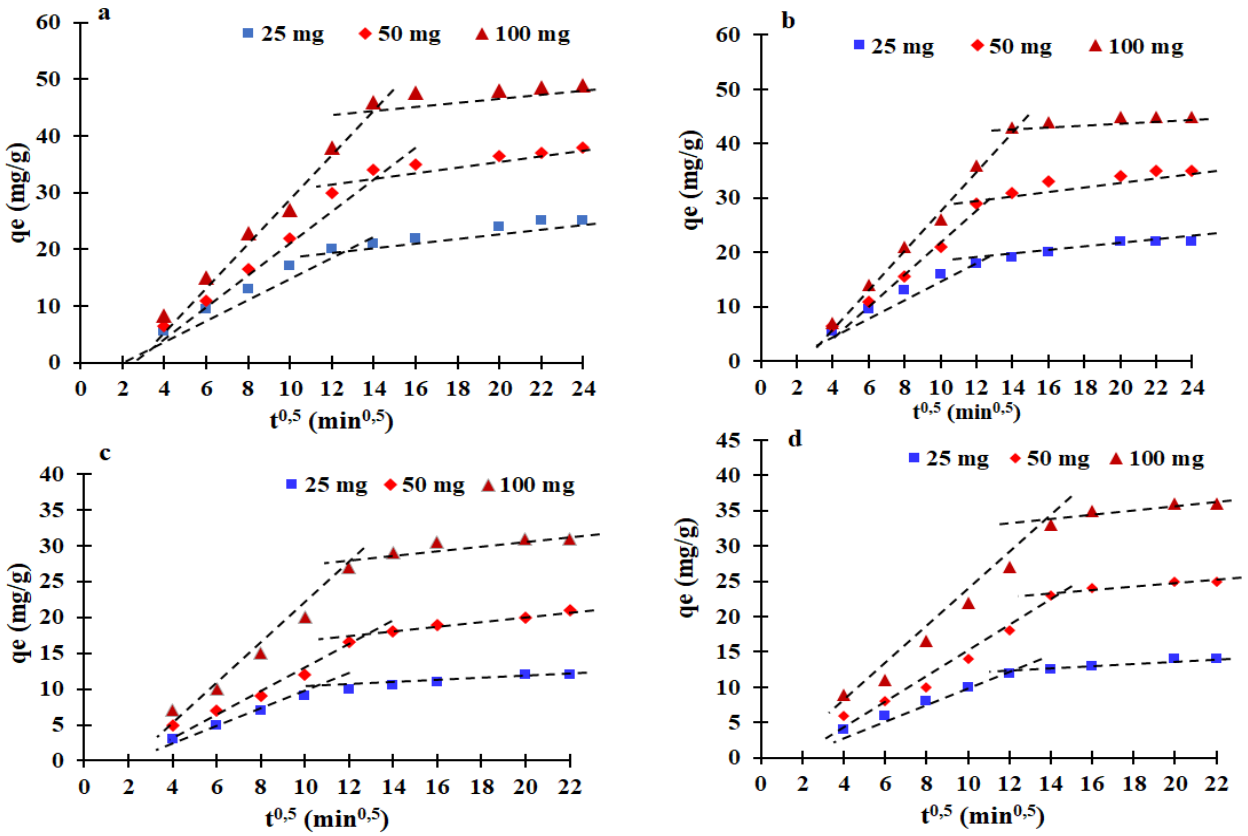

Figure 14: intra-particle diffusion model of the studied anionic (c) EBT, (d) DB71, and cationic (a) MG, (b) MB) dyes onto RPP powder. Conditions: $V_{Solution}$ = 100 mL; pH = 3 (for EBT, DB71) and 7 (for MG, MB). Temperature 25 °C.

Table 4: Thermodynamic parameters calculation of the anionic (EBT, DB71) and cationic (MG, MB) dyes adsorption onto RPP powder. Conditions: C_{dye} = 50 mg.L^{-1}, $V_{Solution}$ = 100 mL; pH = 3 (for EBT, DB71) and 7 (for MG, MB).

	ΔG°(KJ/mol)				ΔS°	ΔH°
Anions	**303 K**	**318 K**	**328 K**	**343 k**	**(J/Kmol)**	**(KJ/mol)**
MG	-10.90	-10.85	-10.82	-10.78	-3.06	-11.83
MB	-11.34	-11.29	-11.26	-11.21	-3.16	-12.30
EBT	-16.83	-16.76	-16.71	-16.64	-4.64	-18.24
DB71	-14.89	-14.80	-14.74	-14.64	-6.12	-16.75

3.5. Adsorption isotherms analysis

The correlation between the adsorption of anionic (EBT, DB71) and cationic (MG, MB) dyes onto RPP powder was studied using mathematical models such as Freundlich, Dubinin-Radushkevich, Sips, Temkin, and Langmuir. According to the results shown in **Table 5**, the Sips, Timkin, Freundlich, and Dubinin-Radushkevich models show a relatively low correlation coefficient R^2, which signifies that the adsorption of the studied dyes is not perfectly in accordance with these models. In contrast, the R^2 coefficients of the Langmuir model (Usman *et al.*, 2022; Haque *et al.*, 2022) are high (0.996-0.998), and thus the adsorption process of anionic (EBT, DB71) and cationic (MG, MB) dyes is perfectly correlated with the Langmuir model with higher q_s of these dyes (41.525 mg.g^{-1} for MG, 40.515 mg.g^{-1} for MB, 31.224 mg.g^{-1} for EBT and 34.536 mg.g^{-1} for DB70) for an initial dye concentration ranging from 25 to 100 mg.L^{-1} and 0.1 g of RPP. In addition, the low values of the affinity constant (K_L) indicate

that the adsorption process of the studied dyes is reversible. On the other hand, the adsorption capacity (K_F) and intensity (n_F) have high values, indicating that the RPP powder has a high adsorption capacity for the dyes. The adsorption energy and heat of sorption (B) values of the dyes calculated by Dubinin-Radushkevich (D-R) and Temkin models are less than 20 kJ/mol, which confirms that the adsorption is mainly physisorption. In summary, based on the results of the isothermal analysis, we can conclude that the Langmuir model is adequate for the description of the adsorption of anionic and cationic dyes on RPP powder, which suggests that this adsorption involves physisorption and chemisorption due to electrostatic interactions between the dyes and the functional groups of RPP (-COOH and -OH).

Table 5: Isotherm parameters of anionic (EBT, DB71) and cationic (MG, MB) dyes adsorption onto RPP powder. Conditions: C_0= 50 mg.L^{-1}, $V_{Solution}$ = 100 mL; pH = 3 (for EBT, DB71) and 7 (for MG, MB). Temperature = 25 °C.

	MG	MB	EBT	DB71
Langmuir				
q_{max} (mg/g)	41.525	40.515	31.224	34.536
K_L (L/mg)	0.062	0.059	0.053	0.055
R^2	0.998	0.997	0.998	0.996
R_L	0.243	0.253	0.273	0.266
Freundlich				
K_F (mg/g) (L/mg)$^{1/n}$	5.643	5.575	5.382	5.475
$1/n_F$	0.624	0.614	0.611	0.608
R^2	0.887	0.879	0.885	0.881
Temkin				
K_T (L/mg)	0.585	0.578	0.554	0.543
B (J/mol)	25.875	24.518	23.852	23.548
R^2	0.921	0.928	0.922	0.919
Dubinin–Radushkevich				
q_s (mg/g)	21.125	20.274	14.547	16.384
K_{DR} (mol^2/J^2)	$3.54.10^{-5}$	$4.28.10^{-5}$	$4.18.10^{-5}$	$5.18.10^{-5}$
E (kJ/mol)	6.254	6.184	5.887	5.715
R^2	0.897	0.889	0.881	0.889
Sips				
q_{max} (mg/g)	38.657	36.851	28.354	30.758
K_S (L.mg^{-1})	0.0884	0.0855	0.0774	0.0811
n	2.958	2.548	1.857	1.985
R^2	0.935	0.945	0.925	0.916
RMS	10.548	11.058	8.584	9.879

3.6. Bibliographic comparison

The adsorption performance of anionic and cationic dyes by RPP powder was evaluated against other adsorbents reported in published works. **Table 6** shows that RPP powder has a higher adsorption capacity than other dye adsorbents. Thus, this comparison with the literature confirms that RPP powder is potentially useful as a practical and efficient adsorbent for the removal of anionic (EBT, DB71) and cationic (MG, MB) dyes.

3.7. Dyes desorption study

The preparation of a practical-use adsorbent for removing anionic (EBT, DB71) and cationic (MG, MB) dyes requires that the adsorbent be able to desorb the fixed dyes in a facile manner. To this end, the regeneration ability of RPP powder was evaluated by treating RPP/anionic dye and RPP/cationic

dye with basic (NaOH: 0.5 M) and acidic (HCl: 0.5 M) solutions, respectively, and at a temperature of 25°C and for different treatment periods, and the desorption rate was calculated for each treatment time.

Table 6: Comparison of the adsorption capacity of dyes on some adsorbents

Adsorbents	Dyes	qe (mg/g)	Removal rate	C_0 of dye	Adsorbent quantity	pH	Ref
chitosan-coated geo textiles based on poly ethylene terephthalate	MG DB71	142 176	91% 95%	0.1 M 0.1 M	10 g 10 g	8 4	(Isaad *et al.*, 2022)
Carbonized waste pomegranate peel.	MG	31.45	99.10	30 mg/L	0.1 g	6	(Gündüz *et al.*, 2017)
Carbonized pomegranate peel activated with HCl	WS	27.32	90.78	30 mg/L	0.1 g	4	(Usman *et al.*, 2022)
Nano-iron oxide-loaded alginate microspheres	MG	-	93.9	10 mg/L	0.1 g	7–8	(Soni *et al.*, 2014)
Cationic Modified Orange Peel Powder	CR	163	-	300 mg/L	0.05 g	3	(Munagapati *et al.*, 2016)
Coir pith	MB	5.87	97 %	20 mg/L	0.3 g	6.9	(Kavitha *et al.*, 2007)
Raw Brazil nut shells	MB	7.81		1100 mg/L	2.5 g	6.5	(De Oliveira Brito *et al.*, 2010)
Orange peel	MB	14.2	-	35 mg/L	0.05 g	4	(Salman *et al.*, 2016)
Banana peel powder	MB	111.11	-	20 mg/L	1 g	5.6	(Moubarak *et al.*, 2014)
Raw pomegranate peel powder	MB	40.5	81 %	50 mg/L	0.1 g		This work
Raw pomegranate peel powder	MG	41.5	83 %	50 mg/L	0.1 g		This work
Raw pomegranate peel powder	EBT	31	62 %	50 mg/L	0.1 g		This work
Raw pomegranate peel powder	D71	34.5	69 %	50 mg/L	0.1 g		This work

WS: Aniline blue dye; CR: Congo Red

Figure 15 shows that generally, the desorption rate of the studied dyes increases with the increase of the treatment time up to a maximum value of 91 % for MG, 89 % for MB, 87 % for DB71, and 85 % for ETB. These maximum desorption values were obtained after a treatment time of min for anionic dyes and min for cationic dyes. The desorption of the dyes is probably related to the rupture of the bonds (van der Waals, electrostatic interaction, hydrogen bonds...) between the fixed dyes and the RPP. Therefore, the desorption of dyes can be easily achieved by varying the pH of the RPP/dye solution and we can conclude that RPP powder is suitable for cationic and anionic dye adsorption with excellent regeneration ability.

3.8. Plausible mechanism of the dye adsorption onto RPP

The results of the zeta potential analysis, adsorption kinetics, and isotherms presented above indicate that the adsorption mechanism of the studied dyes on RPP powder can be explained by (1) the electrostatic interactions (physical adsorption) between the cationic dye (MG, MB) and the adsorbent which is negatively charged (at pH > pH_{pzc}), and the anionic dye (EBT, DB71) and the adsorbent with

positive charges (at pH < pH_{pzc}), as well as by (2) the weak hydrogen bonds between the heteroatoms (oxygen, nitrogen, sulfur atoms) present in the dyes and the hydrogen atoms of the functional groups (-COOH, -OH) available on the adsorbent surface. In addition, the π-π interactions can also be established between the benzene cycles of the studied dyes and the benzene cycles present in the lignin of the RPP powder. In fact, benzene cycles are electron-rich sites, they can produce donor-acceptor stacking interactions between the dyes and RPP as shown in **Figure 16**.

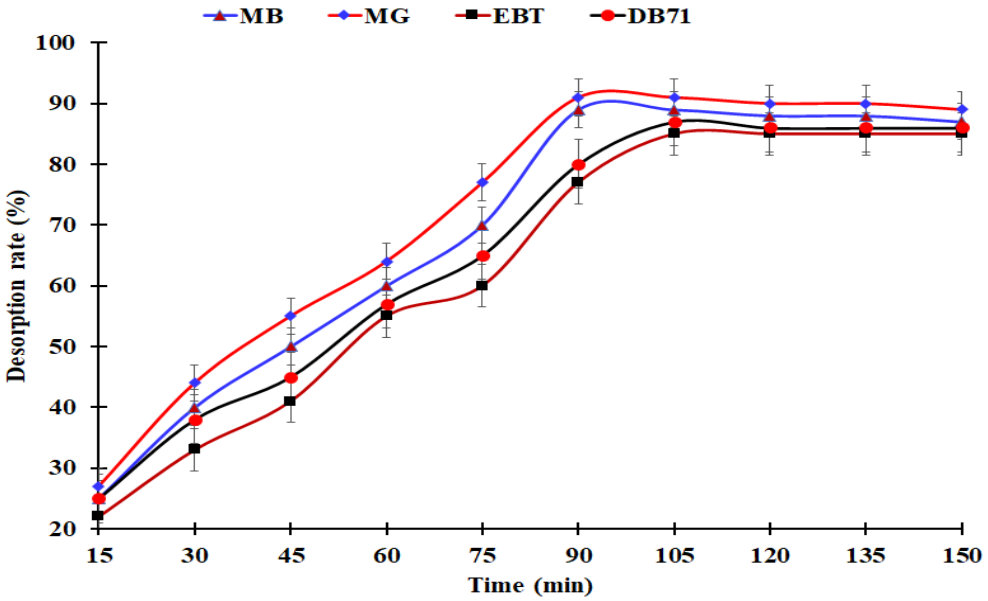

Figure 15: Desorption of the studied anionic (EBT, DB71) and cationic (MG, MB) dyes.

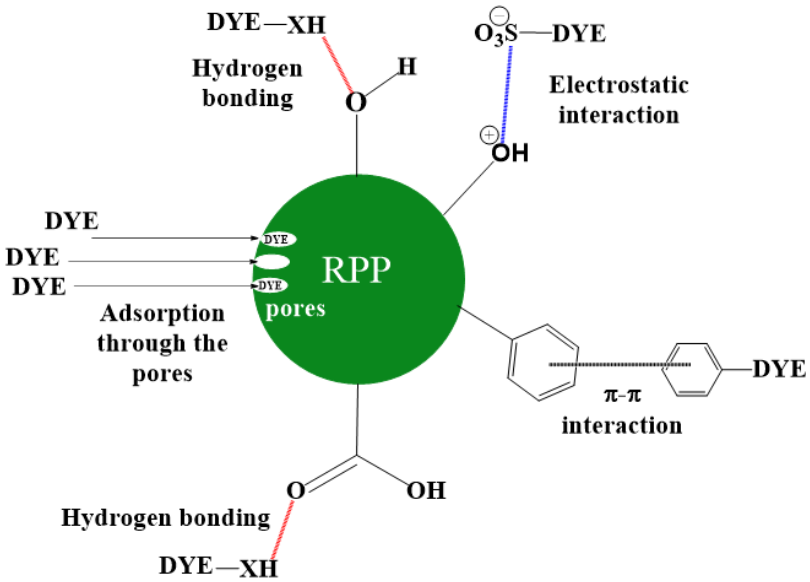

Figure 16: Plausible mechanism of the dye adsorption onto RPP

These findings were also interpreted by Barka *et al.*, 2011, using S. hispanicus biomass by the biosorption yield increased from 15.56 to 85.05% when the biosorbent dosage was increased from 0.1 to 1 g/L for MB and from 14.43 to 72.16% when the biosorbent dosage was increased from 0.1 to 3 g/L for EBT. The observed enhancement biosorption yield with increasing biosorbent concentration could be due to an increase in the number of possible binding sites and surface area of the biosorbent (Bouzidi *et al.*, 2021; El-Naggar *et al.*, 2018; Gong *et al.*, 2005). The SEM images of the resultant

activated carbon prepared from *pomegranate* (Eddebbagh *et al.,* 2016) indicated that the activated carbons have an irregular and heterogeneous surface morphology with a well-developed porous structure. Such pores of different sizes shapes favorized the adsorption of different dies

3.9. Treatment of real water sample

In order to evaluate the adsorption capacity of RPP of anionic (EBT, DB71) and cationic (MG, MB) dyes under real conditions, a solution containing anionic and cationic dyes was prepared with other chemical agents to simulate real conditions as shown in **Table 7**. This solution was treated with RPP powder and the removal rate of dyes was determined. The adsorption results of the studied dyes show that the adsorption capacity of RPP powder decreases in the presence of the other chemical agents (**Figure 17**), but this capacity is still satisfactory in view of the obtained removal rates (47% of MG, 42% of MB, 31% of EBT and 34% of DB71). Therefore, the treatment of textile wastewater, which may contain such chemical agents, can be efficiently performed with RPP powder.

Table 7: Chemical composition of the simulated wastewater

Chemical agents	Concentration ($mg.L^{-1}$)
MG	100
MB	100
EBT	100
DB71	100
NaCl	50
Cu^{2+}	50
Ca^{2+}	50
Fe^{2+}	50
Cr^{6+}	50
Cr^{3+}	50
Humic acid	50
NO_3^-	50
NO_2^-	50
SO_4^-	50
PO_4^{3-}	50

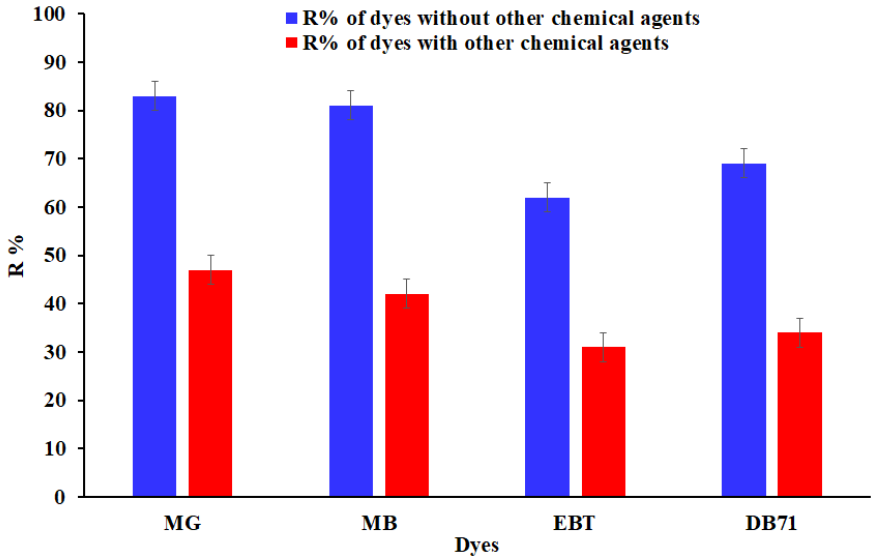

Figure 17: Removal rate (R%) of the anionic (EBT, DB71) and cationic (MG, MB) dyes with and without other chemical agents. Conditions: $V_{Solution}$ = 100 mL; pH= 7 for all studied dyes, RPP quantity = 100 mg, Contact time 60 min, Temperature = 25 °C.

Conclusion

RPP has been valorized as a natural resource-efficient bio-adsorbent for removing anionic (EBT, DB71) and cationic (MG, MB) dyes from a contaminated aqueous solution. Physicochemical and spectroscopic characterizations showed that the RPP powder is constituted of carbon (42.42%), oxygen (51.66%), and hydrogen (5.90%), and presents an amorphous structure with the presence of (-OH) and (-COOH) functions available on the surface of the RPP. Zeta potential study shows that the surface area of RPP shows pH_{pzc}= 5.6 and this surface area is negative at pH< pH_{pzc} and positive at pH> pH_{pzc}. Surface analysis by B.E.T. indicates that the specific surface area, total volume, and average pore diameter of RPP particles are about 1.105 $m^2.g^{-1}$, 0.0017 $cm^3.g^{-1}$, and 71.45 Å, respectively, for powders of 250 µm in size. The adsorption of the studied dyes on RPP was confirmed by XPS spectroscopy of RPP and RPP/dye by showing new peaks attributed to N1s and S2p of the studied dyes in the XPS spectrum of RPP. The experimental results of adsorption showed that RPP has a high efficiency to remove the studied anionic and cationic dyes which reach an adsorption capacity of 81% for MB and 83% for MG obtained at pH= 7, and 69% for DB71 and 62% for EBT at pH3, during 60 min as contact time, for an initial dye concentration of 50 $mg.L^{-1}$ and an amount of RPP of 0.1 g at a temperature of 25 °C. The results of the isothermal analysis indicate that the Langmuir model is appropriate to describe the adsorption of the studied dyes by RPP, which involves physisorption and chemisorption processes, and the sorption kinetic data are consistent with the pseudo-second-order kinetic model. The adsorption mechanism is explained by the electrostatic interactions between the opposite charges of RPP and dyes as a function of solution pH and pHpzc, as well as the π-π interaction established between the benzene cycles of the dyes and the benzene cycles of the lignin portion of the RPP powder, and also by the H-bonds. The desorption of anionic (EBT, DB71) and cationic (MG, MB) dyes was established by treating RPP/anionic dye and RPP/cationic dye with NaOH (0.5 M) and HCl (0.5 M) solutions, respectively and the results obtained showed that 91% of MG, 89% of MB, 87% of DB71 and 85% of ETB could be desorbed from RPP powder. Finally, the RPP adsorption experiment on a solution simulating real conditions shows a promising application in wastewater treatment.

Disclosure statement: *Conflict of Interest:* The authors declare that there are no conflicts of interest.
Compliance with Ethical Standards: This article does not contain any studies involving human or animal subjects.

References

Aaddouz M., Azzaoui K., Akartasse N., Mejdoubi E., Hammouti B., Taleb M., Sabbahi R., Alshahateet S.F. (2023). Removal of Methylene Blue from aqueous solution by adsorption onto hydroxyapatite nanoparticles, *Journal of Molecular Structure*, 1288, 135807, doi.org/10.1016/j.molstruc.2023.135807

Ahmad, I., Aalam, G., Amir, M., Chakravarty, A., Ali, S. W., Ikram, S. (2022). Development of highly efficient magnetically recyclable Cu^{2+}/Cu^0 nano-photocatalyst and its enhanced catalytic performance for the degradation of organic contaminations. *Sci. Total Environ*, 846, 157154.

Akram, M., Gao, B., Pan, J., Khan, R., Inam, M. A., Xu, X., Guo, K., Yue, Q. (2022). Enhanced removal of phosphate using pomegranate peel-modified nickel-lanthanum hydroxide. *Sci. Total Environ,* 809, 151181. https://doi.org/10.1016/j.scitotenv.2021.151181

Al-Onazi, W. A., Ali, M. H. H., Al-Garni, T. (2021). Using Pomegranate Peel and Date Pit Activated Carbon for the Removal of Cadmium and Lead Ions from Aqueous Solution. *J. Chem*, 2021, e5514118. https://doi.org/10.1155/2021/5514118

Anliker R. (1979). Ecotoxicology of dyestuffs-A joint effort by industry. *Ecotoxicol. Environ. Saf*, 3(1), 59-74.

Athawale, A., Bokare, A., Singh, H., Nguyen, V.-H., Vo, D.-V. N., Kumar, D., Sharma, A. (2020). Synthesis of Ag_2O coated TiO_2 nanoparticles by sonochemically activated methods for enhanced photocatalytic activities. *Top Catal*, *63*, 1056–1065.

Bauer C., Jacques, P., Kalt, A. (2001). Photooxidation of an azo dye induced by visible light incident on the surface of TiO_2. *J. Photochem. Photobiol. A*, *140*(1), 87–92.

Bellahsen, N., Varga, G., Halyag, N., Kertész, S., Tombácz, E., Hodúr, C. (2021). Pomegranate peel as a new low-cost adsorbent for ammonium removal. *Int J Environ Sci Technol*, *18*(3), 711–722. https://doi.org/10.1007/s13762-020-02863-1

Ben-Ali, S. (2021). Application of Raw and Modified Pomegranate Peel for Wastewater Treatment: A Literature Overview and Analysis. *Int. J. Chem. Eng*, *2021*, e8840907. https://doi.org/10.1155/2021/8840907

Ben-Ali, S., Jaouali, I., Souissi-Najar, S., Ouederni, A. (2017). Characterization and adsorption capacity of raw pomegranate peel biosorbent for copper removal. *J. Clean. Prod*, *142*, 3809–3821. https://doi.org/10.1016/j.jclepro.2016.10.081

Bianchini, R., Bonanni, M., Corsi, M., Infantino, A. S. (2012). Viable and straightforward approach to the preparation of water soluble pyrazol-5-one derivatives through glycoconjugation. *Tetrahedron*, *68*(41), 8636–8644. https://doi.org/10.1016/j.tet.2012.07.074

Bianchini, R., Catelani, G., Cecconi, R., D'Andrea, F., Guazzelli, L., Isaad, J., Rolla, M. (2008). Ethereal Glycoconjugated Azodyes (GADs): A New Group of Water-Soluble, Naturalised Dyes. *EurJOC*, *2008*(3), 444–454. https://doi.org/10.1002/ejoc.200700632

Bianchini, R., Catelani, G., Frino, E., Isaad, J., Rollaa, M. (2007). Lactose to naturalize textile dyes. *BioResources*, *2*(4), 630–637.

Barka N., Abdennouri M., EL Makhfouk M. (2011), Removal of Methylene Blue and Eriochrome Black T from aqueous solutions by biosorption on Scolymus hispanicus L.: Kinetics, equilibrium and thermodynamics, *Journal of the Taiwan Institute of Chemical Engineers*, 42(2), 320-326, doi:10.1016/j.jtice.2010.07.004

Bouzidi A., Djedid M., Ad C., Benalia M., Hafez B., Elmsellem H. (2021). Biosorption of Co (II) ions from aqueous solutions using selected local Luffa Cylindrica: Adsorption and characterization studies, *Mor. J. Chem.* 9 N°1, 156-167, https://doi.org/10.48317/IMIST.PRSM/morjchem-v9i1.23215

Chung, K.-T., Fulk, G. E., Andrews, A. W. (1981). Mutagenicity testing of some commonly used dyes. *Appl. Environ. Microbiol. 42*(4), 641–648.

Combes R. D., Haveland-Smith R.B. (1982). A review of the genotoxicity of food, drug and cosmetic colours and other azo, triphenylmethane and xanthene dyes. *Mutat Res*. 98(2), 101-248. doi: 10.1016/0165-1110(82)90015-x. PMID: 7043261

Cui, M.-H., Liu, W.-Z., Tang, Z.-E., Cui, D. (2021). Recent advancements in azo dye decolorization in bio-electrochemical systems (BESs): Insights into decolorization mechanism and practical application. *Water Res, 203*, 117512.

Dassanayake, R. S., Acharya, S., Abidi, N. (2021). Recent Advances in Biopolymer-Based Dye Removal Technologies. *Molecules*, *26*(15), Article 15. https://doi.org/10.3390/molecules26154697

De Oliveira Brito, S. M., Andrade, H. M. C., Soares, L. F., de Azevedo, R. P. (2010). Brazil nut shells as a new biosorbent to remove methylene blue and indigo carmine from aqueous solutions. *J. Hazard. Mater*, *174*(1), 84–92. https://doi.org/10.1016/j.jhazmat.2009.09.020

Druet, J., El Achari, A., Isaad, J. (2015). Efficient removal of heavy metals from aqueous solution by chitosan-coated geotextiles based on polyethylene terephthalate. *Res. Chem. Intermed*, *41*(11), 8855–8876. https://doi.org/10.1007/s11164-015-1933-5

Dahri, M.K., Kooh, M., Lim, L. (2018) Casuarina equisetifolia cone as sustainable adsorbent for removal of Malachite green dye from aqueous solution using batch experiment method, *Moroccan Journal of Chemistry,* 6(3), pp. 480-491, https://doi.org/10.48317/IMIST.PRSM/morjchem-v6i3.8018

Eddebbagh M., Abourriche A., Berrada M., Ben Zina M. and Bennamara A. (2016) Adsorbent material from *pomegranate* (Punica granatum) leaves: Optimization on removal of methylene blue using response surface methodology, *J. Mater. Environ. Sci.* 7 (6), 2021-2033

El Badraoui, A., Miyah, Y., Nahali, L., Zerrouq, F., El Khazzan, B. (2019) Fast adsorption for removal of methylene blue from aqueuous solutions using of local clay, *Moroccan Journal of Chemistr*y 7(3), pp. 416-423, https://doi.org/10.48317/IMIST.PRSM/morjchem-v7i3.16742

El Hammari L., Latifi S., Saoiabi S., Saoiabi A., Azzaoui K., Hammouti B., Chetouani A., Sabbahi R. (2022), Toxic heavy metals removal from river water using a porous phospho-calcic hydroxyapatite, *Mor. J. Chem.* 10(1), 62-72, https://doi.org/10.48317/IMIST.PRSM/morjchem-v10i1.31752

El-Naggar N.E., Hamouda R.A., Mousa I.E., Abdel-Hamid M.S., Rabei N.H. (2018) Biosorption optimization, characterization, immobilization and application of Gelidium amansii biomass for complete Pb2+ removal from aqueous solutions. *Sci Rep.,* 8(1), 13456. doi: 10.1038/s41598-018-31660-7

Elsherif K.M., El-Dali A., Ewlad-Ahmed A. M., Treban A. A., Alqadhi H., Alkarewi S. (2022) Kinetics and Isotherms Studies of Safranin Adsorption onto Two Surfaces Prepared from Orange Peels, *Mor. J. Chem.* 10N°4, 639-651, https://doi.org/10.48317/IMIST.PRSM/morjchem-v11i1.32137

Eltaweil, A. S., El-Monaem, E. M. A., Elshishini, H. M., El-Aqapa, H. G., Hosny, M., Abdelfatah, A. M., Ahmed, M. S., Hammad, E. N., El-Subruiti, G. M., Fawzy, M., Omer, A. M. (2022). Recent developments in alginate-based adsorbents for removing phosphate ions from wastewater: A review. *RSC Adv*, *12*(13), 8228–8248. https://doi.org/10.1039/D1RA09193J

Eltaweil, A. S., Omer, A. M., El-Aqapa, H. G., Gaber, N. M., Attia, N. F., El-Subruiti, G. M., Mohy-Eldin, M. S., Abd El-Monaem, E. M. (2021). Chitosan based adsorbents for the removal of phosphate and nitrate: A critical review. *Carbohydr. Polym*, *274*, 118671. https://doi.org/10.1016/j.carbpol.2021.118671

Gong R., Ding Y., Liu H., Chen Q., Liu Z. (2005) Lead Biosorption and Desorption by Intact and Pretreated Spirulina Maxima Biomass, *Chemosphere,* 58, p. 125

Gündüz, F., Bayrak, B. (2017). Biosorption of malachite green from an aqueous solution using pomegranate peel: Equilibrium modelling, kinetic and thermodynamic studies. *J. Mol. Liq*, *243*, 790–798. https://doi.org/10.1016/j.molliq.2017.08.095

Hamous, H., Khenifi, A., Orts, F., Bonastre, J., Cases, F. (2021). Carbon textiles electrodes modified with RGO and Pt nanoparticles used for electrochemical treatment of azo dye. *J. Electroanal. Chem*, *887*, 115154.

Haque, A. N. M. A., Sultana, N., Sayem, A. S. M., Smriti, S. A. (2022). Sustainable Adsorbents from Plant-Derived Agricultural Wastes for Anionic Dye Removal: A Review. *Sustainability*, *14*(17), Article 17. https://doi.org/10.3390/su141711098

He, L., Chen, Y., Li, Y., Sun, F., Zhao, Y., Yang, S. (2022). Adsorption of Congo red and tetracycline onto water treatment sludge biochar: Characterisation, kinetic, equilibrium and thermodynamic study. *Water Sci. Technol*, *85*(6), 1936–1951.

Ho, Y. S., McKay, G. (1999). Pseudo-second order model for sorption processes. *Process Biochem*, *34*(5), 451–465. https://doi.org/10.1016/S0032-9592(98)00112-5

Hu, S., Yuan, J., Tang, S., Luo, D., Shen, Q., Qin, Y., Zhou, J., Tang, Q., Chen, S., Luo, X. (2022). Perovskite-type SrFeO3/g-C3N4 S-scheme photocatalyst for enhanced degradation of Acid Red B. *Opt. Mater*, *132*, 112760.

Hunger, K. (2003). Dyes, general survey. *Industrial Dyes: Chemistry, Properties, Applications, Wiley Subscription Services, Inc., A Wiley Company, Frankfurt*, 1–10.

International Agency for Research on, IARC (International Agency for research on cancer. (1982). Some industrial chemicals and dyestuffs. In *Some industrial chemicals and dyestuffs* (pp. 416–416). https://pesquisa.bvsalud.org/portal/resource/pt/mis-17352

Isaad, J. (2013). Highly water-soluble dyes based on pyrazolone derivatives of carbohydrates. *Tetrahedron*, *69*(10), 2239–2250. https://doi.org/10.1016/j.tet.2013.01.038

Isaad, J., El Achari, A. (2020). Synthesis and Spectroscopic Characterization of Water Soluble Triazene Dyes Based on Glyco-conjugated Pyrazolone Derivatives Catalyzed by an Acidic Ionic Liquid Supported on Silica-Coated Magnetite Nanoparticles. *Chem. Afr*, *3*(4), 889–899. https://doi.org/10.1007/s42250-020-00186-9

Isaad, J., El Achari, A. (2021). Preparation of aminated magnetite / SiO_2 / chitosan core-shell nanoparticles for efficient adsorption of nitrate and phosphate anions in water. *Int. J. Environ. Anal. Chem*, *0*(0), 1–30. https://doi.org/10.1080/03067319.2021.2014468

Isaad, J., El Achari, A. (2022). Chitosan-coated nonwoven polyethylene terephthalate material for efficient removal of cationic and anionic dyes from aqueous solution. *Int. J. Environ. Anal. Chem*, *102*(17), 5472–5494.

Isaad, J., Perwuelz, A. (2010). New color chemosensors for cyanide based on water-soluble azo dyes. *Tetrahedron Lett*, *51*(44), 5810–5814. https://doi.org/10.1016/j.tetlet.2010.08.098

Kankou M. S.'A., N'diaye A. D., Hammouti B., Kaya S. and Fekhaoui M. (2021) Ultrasound-assisted adsorption of Methyl Parathion using commercial Granular Activated Carbon from aqueous solution, *Mor. J. Chem.* 9(4), 832-842

Kavitha, D., Namasivayam, C. (2007). Experimental and kinetic studies on methylene blue adsorption by coir pith carbon. *Bioresour. Technol*, *98*(1), 14–21. https://doi.org/10.1016/j.biortech.2005.12.008

Kouar J., Ould Bellahcen T., Elamrani A., Cherif A., Kamil N. (2021) Removal of Eriochrome Black T dye from aqueous solutions by using nano-crystalline calcium phosphate tricalcic apatitic, *Mor. J. Chem.* 9(3), 715-725, https://doi.org/10.48317/IMIST.PRSM/morjchem-v9i3.26577

Kyzas, G. Z., Bikiaris, D. N., Mitropoulos, A. C. (2017). Chitosan adsorbents for dye removal: A review. *Polym. Int*, *66*(12), 1800–1811. https://doi.org/10.1002/pi.5467

Lee, J. H., Lee, Y., Bathula, C., Kadam, A. N., Lee, S.-W. (2022). A zero-dimensional/two-dimensional Ag–Ag_2S–CdS plasmonic nanohybrid for rapid photodegradation of organic pollutants by solar light. *Chemosphere*, *296*, 133973.

Li, P. H. Y., Bruce, R. L., Hobday, M. D. (1999). A pseudo-first-order rate model for the adsorption of an organic adsorbate in aqueous solution. *J. Chem. Technol. Biotechnol*, *74*(1), 55–59. https://doi.org/10.1002/(SICI)1097-4660(199901)74:1<55::AID-JCTB984>3.0.CO;2-D

Li, X., Zhang, J., Qin, Y., Zhang, X., Zou, W., Ding, L., Zhou, M. (2022). Enhanced removal of organic contaminants by novel iron–carbon and premagnetization: Performance and enhancement mechanism. *Chemosphere*, *303*, 135060.

Li, Y., Yi, H., Li, M., Ge, M., Yao, D. (2022). Synchronous degradation and decolorization of colored poly (ethylene terephthalate) fabrics for the synthesis of high-purity terephthalic acid. *J. Clean. Prod*, *366*, 132985.

Liao, X., Cao, J., Lei, M., Zhang, C., Hu, L. (2022). Impact of manganese sulfide (MnS) oxygenation-induced oxidization on aqueous organic contaminants: Insight into the role of the hydroxyl radical (HO·). *Sci. Total Environ*, *840*, 156702.

Liu, D., Liang, H., Xu, T., Bai, J., Li, C. (2022). Construction of ternary hollow TiO_2-ZnS@ ZnO heterostructure with enhanced visible-light photoactivity. *J. Mol. Struct*, *1248*, 131493.

Liu, Q., Wang, J., Duan, C., Wang, T., Zhou, Y. (2022). A novel cationic graphene-modified cyclodextrin adsorbent with enhanced removal performance of organic micropollutants and high antibacterial activity. *J. Hazard. Mater*, *426*, 128074.

Loubna, N., Miyah, Y., Ouissal, A., (...), Bouchta, E.K., Farid, Z. (2019) Kinetic and thermodynamicstudy of the adsorption of twodyes: Brilliant green and eriochrome black T using a natural adsorbent "sugarcane bagasse, *Mor. J. Chem.,* 7(4), 715-726, /doi:10.48317/IMIST.PRSM/morjchem-v7i4.17182

Malik, D. S., Jain, C. K., Yadav, A. K. (2017). Removal of heavy metals from emerging cellulosic low-cost adsorbents: A review. *Appl. Water Sci, 7*(5), 2113–2136. https://doi.org/10.1007/s13201-016-0401-8

Medjahed, K., Tennouga, L., Mansri, A., Chetouani, A., Hammouti B., Desbrières, J. (2013), Interaction between poly(4-vinylpyridine-graft-bromodecane) and textile blue basic dye by spectrophotometric study, *Res. Chem. Intermed.,* 39 N°7, 3199-3208.

Moubarak, F., Atmani, R., Maghri, I., Elkouali, M., Talbi, M., Bouamrani, M. L., Salouhi, M., Kenz, A. (2014). Elimination of Methylene Blue Dye with Natural Adsorbent (Banana Peels Powder). *Glob. J. Sci. Front. Res,* 14, 38-44.

Muhammad A. S., Abdurrahman M. A. (2020) Adsorption of Methylene blue onto modified Agricultural waste, *Mor. J. Chem.* 8N°2, 412-427, https://doi.org/10.48317/IMIST.PRSM/morjchem-v8i2.16692

Munagapati, V. S., Kim, D.-S. (2016). Adsorption of anionic azo dye Congo Red from aqueous solution by Cationic Modified Orange Peel Powder. *J. Mol. Liq*, *220*, 540–548. doi.org/10.1016/j.molliq.2016.04.119

Salman, T. A., Ali, M. I. (2016). Potential Application of Natural and Modified Orange Peel as an Eco–friendly Adsorbent for Methylene Blue Dye. *Iraqi J. Sci*, *57*(1A), Article 1A.

Salmani, M.H., Abedi, M., Mozaffari, S.A., Mahvi, A.H., Sheibani, A., Jalili, M. (2021). Simultaneous reduction and adsorption of arsenite anions by green synthesis of iron nanoparticles using pomegranate peel extract. *J. Environ. Health Sci. Eng,* 19, 603–612

Sheth, Y., Dharaskar, S., Khalid, M., Sonawane, S. (2021). An environment-friendly approach for heavy metal removal from industrial wastewater using chitosan-based biosorbent: A review. *Sustain. Energy Technol. Assess*, *43*, 100951. https://doi.org/10.1016/j.seta.2020.100951

Shokri, A. (2022). Employing electro-peroxone process for degradation of Acid Red 88 in aqueous environment by Central Composite Design: A new kinetic study and energy consumption. *Chemosphere*, *296*, 133817.

Soni, A., Tiwari, A., Bajpai, A. K. (2014). Removal of malachite green from aqueous solution using nano-iron oxide-loaded alginate microspheres: Batch and column studies. *Res. Chem. Intermed*, *40*(3), 913–930. https://doi.org/10.1007/s11164-012-1011-1

Sun, L., Mo, Y., Zhang, L. (2022). A mini-review on bio-electrochemical systems for the treatment of azo dye wastewater: State-of-the-art and future prospects. *Chemosphere*, 294, 133801.

Tsuda, S., Matsusaka, N., Madarame, H., Ueno, S., Susa, N., Ishida, K., Kawamura, N., Sekihashi, K., Sasaki, Y. F. (2000). The comet assay in eight mouse organs: Results with 24 azo compounds. *Mutat Res Genet Toxicol Environ Mutagen*, *465*(1–2), 11–26.

Usman, M. A., Aftab, R. A., Zaidi, S., Adnan, S. M., Rao, R. a. K. (2022). Adsorption of aniline blue dye on activated pomegranate peel: Equilibrium, kinetics, thermodynamics, and support vector regression modelling. *Int J Environ Sci Technol*, *19*(9), 8351–8368. https://doi.org/10.1007/s13762-021-03571-0

Vinod, V. T. P., Sashidhar, R. B., Sukumar, A. A. (2010). Competitive adsorption of toxic heavy metal contaminants by gum kondagogu (Cochlospermum gossypium): A natural hydrocolloid. *Colloids Surf. B 75*(2), 490–495. https://doi.org/10.1016/j.colsurfb.2009.09.023

Wawrzkiewicz, M., Podkościelna, B., Jesionowski, T., Klapiszewski, Ł. (2022). Functionalized microspheres with co-participated lignin hybrids as a novel sorbents for toxic CI Basic Yellow 2 and CI Basic Blue 3 dyes removal from textile sewage. *Ind. Crops Prod 180*, 114785.

Xiang, D., Lu, S., Ma, Y., Zhao, L. (2022). Synergistic photocatalysis-fenton reaction of flower-shaped CeO2/Fe3O4 magnetic catalyst for decolorization of high concentration congo red dye. *Colloids Surf. A: Physicochem. Eng. Asp*, *647*, 129021.

Xu, D., Kong, Q., Wang, X., Lou, T. (2022). Preparation of carboxymethyl cellulose/chitosan-CuO giant vesicles for the adsorption and catalytic degradation of dyes. *Carbohydr. Polym*, *291*, 119630.

Yagub, M. T., Sen, T. K., Afroze, S., Ang, H. M. (2014). Dye and its removal from aqueous solution by adsorption: A review. *Adv. Colloid Interface Sci*, *209*, 172–184.

Zhao, C., Liu, G., Tan, Q., Gao, M., Chen, G., Huang, X., Xu, X., Li, L., Wang, J., Zhang, Y., Xu, D. (2023). Polysaccharide-based biopolymer hydrogels for heavy metal detection and adsorption. *J. Adv. Res*, *44*, 53–70. https://doi.org/10.1016/j.jare.2022.04.005

Zollinger, H. (2003). Color Chemistry: Synthesis. *Properties and Application of Organic Dyes and Pigment, New York: Willey-VCH*.

(2023) ; https://revues.imist.ma/index.php/morjchem/index